Journal of Electrical Engineering and Automation (ISSN: 2582-3051)
www.irojournals.com/iroeea/

Decentralized Control Strategy for Voltage Regulation in Islanded DC Microgrids

Thanveer Nishath S.[1], Amuthan G.[2]

Electrical and Electronics Engineering, Government College of Technology, Anna University, Coimbatore, India.

Email: [1]thanveer0028@gmail.com, [2]gamuthan@gct.ac.in

Abstract

Every distributed energy resource (DER), including battery systems and solar panels, has local controllers that respond to variations in frequency and voltage to modify power generation in order to maintain voltage stability. In this context, traditional droop control is commonly used to control variable states of charge (SoC) in battery energy storage systems (BESS) and to enable decentralized control for load sharing among distributed generator (DG) units. While grid integration provides increased flexibility and resilience, decentralizing energy management allows the system to optimize local energy resources independently, creating a resilient and flexible system that can react to changing grid conditions.

Keywords: Distributed Energy Resource (DER), Distributed Generator (DG), State of Charge (SoC), Battery Energy Storage Systems (BESS) Units, Decentralizing Energy Management.

1. Introduction

A stand-alone power system that functions separately from the main grid is known as an islanded DC microgrid. It generates, distributes, and consumes power using direct current (DC). The system must manage its energy resources independently since it is "islanded" if it is physically or electrically cut off from the wider grid [1]. DC microgrids are becoming more popular than conventional AC microgrids as RESs are being used more frequently [2]. This trend has a number of benefits, such as the elimination of frequency-related problems and harmonics, the removal of the need for synchronization in islanded mode, and the removal of difficulties with reactive power control. However, because renewable energy sources are

DOI: https://doi.org/10.36548/jeea.2025.2.001
Received: 22.04.2025, received in revised form: 20.05.2025, accepted: 03.06.2025, published: 13.06.2025

variable, incorporating them into DC microgrids may pose reliability issues. Fossil fuel-based generators, like gas or diesel units, are frequently included to improve system reliability [3]. The stability of DC microgrids can be greatly increased by incorporating multiple energy storage systems, such as batteries and supercapacitors, but doing so also adds complexity to control and management, creating new problems [4], [5]. Without the use of efficient power management techniques, DC microgrids' efficiency is still limited, even though adding fossil fuel-based generators can somewhat increase their dependability [6].

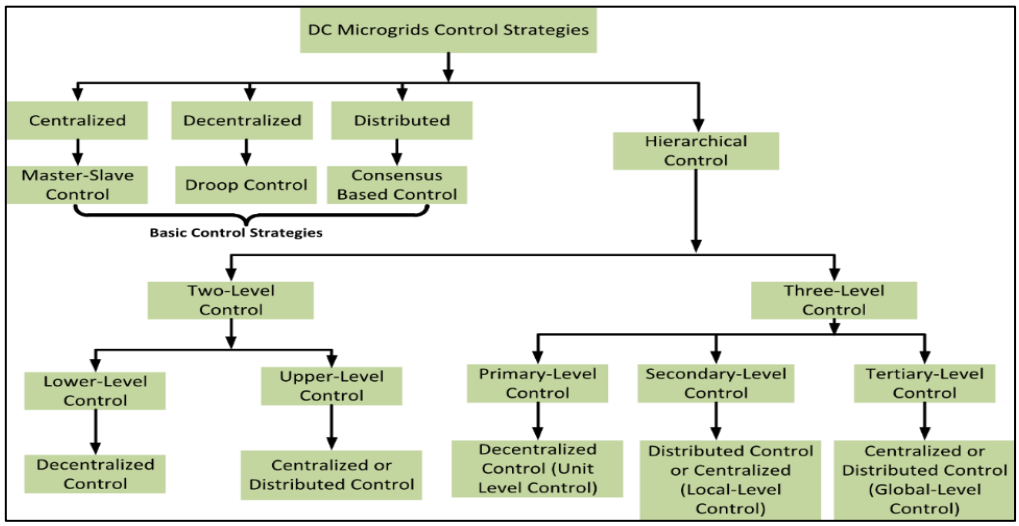

Figure 1. Typical Flowchart for Types of Control Strategies [17]

In DC microgrids, a decentralized control strategy is one in which each distributed energy resource (DER) or converter runs independently and only uses local measurements, like voltage and current, to control its output. The units no longer need to coordinate centrally or communicate extensively with one another thanks to this methodology [7].

2. Existing System

Droop control, shown in Figure 2, has long been used as a decentralized method to control load-sharing between DG and BESS, allowing for independent operation and the smooth addition of new DG units. Droop control is straightforward, but it has drawbacks like unregulated voltage and imprecise load-sharing that can negatively impact system performance as a whole. BESS is essential for maintaining a balance between the supply and demand for energy, especially when renewable energy production is both steady and variable. As explained in [8], energy management in islanded microgrids presents considerable difficulties, requiring

efficient control mechanisms to guarantee steady and dependable power delivery. In order to overcome these difficulties, a droop control system that permits decentralized power sharing and voltage regulation is described in References [9]–[12]. This method improves overall energy management efficiency by integrating the state-of-charge (SoC) of BESS into a modified droop control strategy.

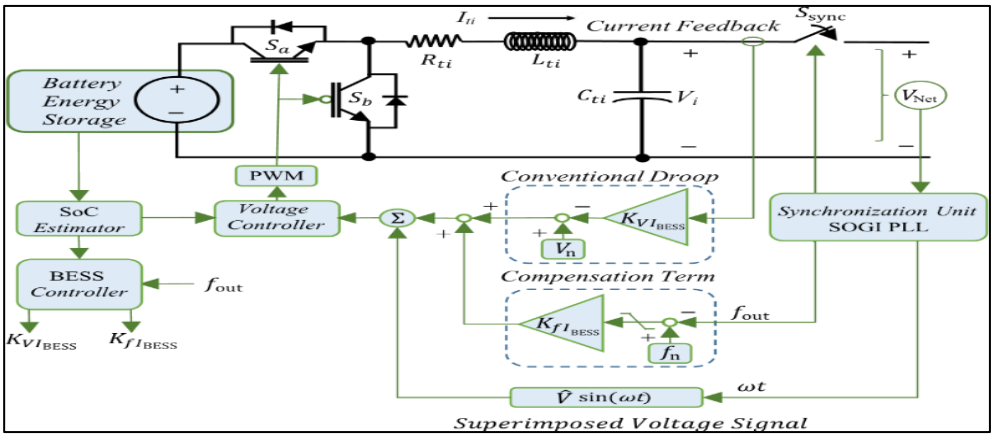

Figure 2. Existing System Block Diagram for BESS Unit

Through software simulations using Piecewise Linear Electrical Circuit Simulation, the effectiveness of the suggested control system in guaranteeing accurate power sharing and voltage regulation has been confirmed. Depending on their state-of-charge (SoC), this system currently uses BESS as bidirectional distributed generators (DGs) for load-sharing. Through a decentralized approach, this configuration guarantees precise load distribution and controlled voltage regulation within an islanded DC microgrid. While the secondary distributed generator unit and battery storage control the frequency and phase of the AC voltage, the primary distributed generator unit superimposes the AC voltage on the low DC voltage. Through the output current, the main unit modifies frequency while maintaining a constant DC voltage. By storing excess energy when it becomes available and making sure a sufficient energy reserve is maintained, BESS units help the grid during times of peak demand and contribute to overall stability by controlling energy storage in accordance with load demands and SoC. A planned droop control technique is used to efficiently manage energy within the Battery Energy Storage System (BESS) unit. Using this method, the battery storage controller fixes the coefficients KVIBESS and KfIBESS. The three operating modes of the BESS—charging, floating, and discharging—are used to modify these coefficients. When the frequency drop

(Δfout) drops below the charging threshold (Δfch), the charging mode is triggered. The BESS unit does not share power when it is in fluctuating mode. When the frequency drop surpasses the discharging threshold (Δfdch), usually in high-load situations, the discharge mode is activated. In order to adjust the recovery time and sensitivity to variations in the state of charge (SoC) level and power sharing, the BESS unit adjusts the droop constants based on its charging and discharging ratings using parameters α and β. A lower SoC puts the BESS into charging mode, essentially turning it into a load for the DC microgrid, while a higher SoC increases load sharing during discharging mode. The BESS unit switches to discharging mode and uses conventional droop control for load-sharing if the frequency deviation exceeds the maximum permitted drop (Δfmax), which indicates an overloaded or broken main distributed generator (DG) unit. By keeping the frequency below a certain threshold, the DG units stay in sync, guaranteeing that the DC microgrid continues to operate normally. A backup secondary distributed generator takes over as the primary distributed generator in the event that the primary DG unit fails. A direct current microgrid with two distributed generators, a main distributed generator, and energy storage is investigated using the current control scheme in order to assess the system's stability during the charging and discharging phases. Kirchhoff's current and voltage laws have been used to create a state-space model of the direct current microgrid. The load voltage at a mutual connection point, the source voltage of the generated direct current, the current in the system's localized load, and the distribution network's line current are important variables in this model. Load currents, filter currents, and other pertinent system parameters were taken into consideration when calculating the system's output current and the distributed generator's destination voltage.

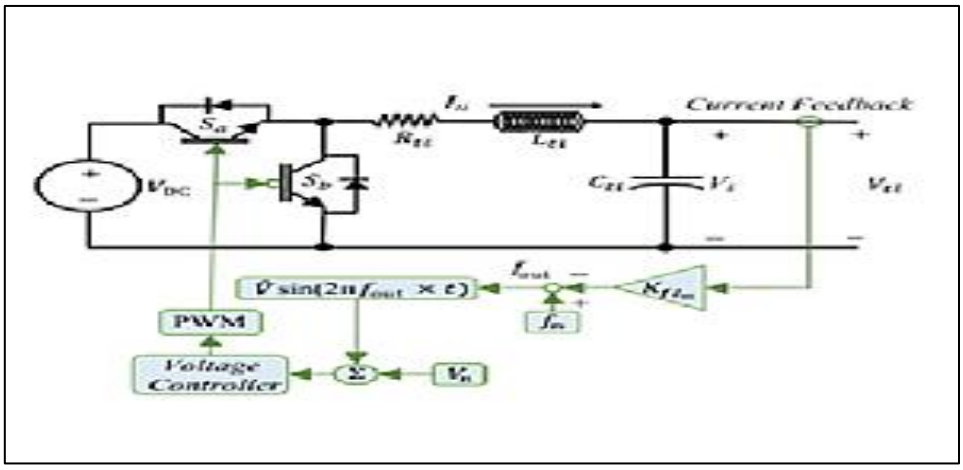

Figure 3. Structure of Main DG Unit and

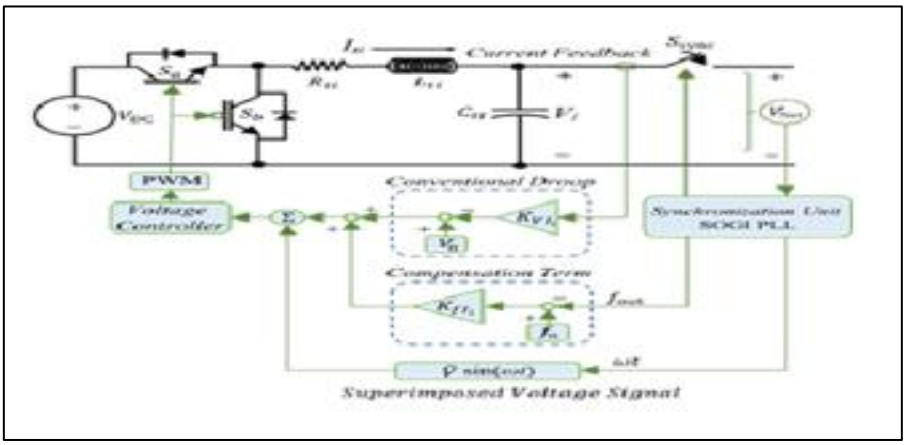

Figure 4. Slave DG Unit

Figures 3 and 4 The alternating current voltage was superimposed on top of the current direct current voltage because of a renewable distributed generator, also referred to as a main distributed generator. The remaining renewable distributed generators and energy storage systems were used to monitor the system's frequency rate and the degree of phase shifting of the overlaid alternating current voltage [14]. Regardless of the load conditions, the main distributed generator's output voltage stays constant at a direct current level. The frequency rate droop control method is used to regulate an overlaid alternating current voltage [15]. The main distributed generator applies an alternating current voltage, whose frequency is dependent on the load, on top of the current direct current voltage. By adding a compensated voltage for secondary distributed generators based on an overlaid alternating current voltage, the proposed system improves upon the conventional droop mechanism. Voltage must be adjusted for energy storage based on the battery's charge level. Consequently, the system provides decentralized voltage regulation and meets energy management requirements [16].

2.1 Drawbacks of Existing System

Real-world variables, like aging components, environmental conditions, and interactions between DG units, can affect system performance. The integration of overlaid AC voltage and the use of sophisticated hardware make the current system more complex and require advanced monitoring and control. The BESS unit must be properly sized and maintained for the system to function effectively, especially during times of high demand or in the event of a fault.

3. Proposed System

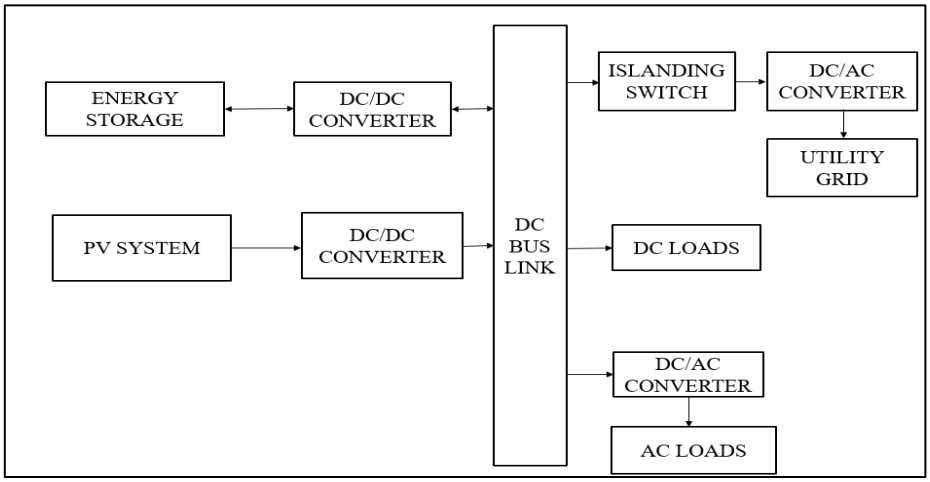

Figure 5. Block Diagram for Proposed Work

With an emphasis on distributed control to maximize energy generation, storage, and consumption, this work (figure 5) suggests a decentralized control approach for energy management and voltage regulation in a photovoltaic (PV)-based energy system. To condition DC power, the PV system uses a SEPIC converter. For effective power distribution, a PWM generator uses an MPPT algorithm. The battery system is managed by a bidirectional dc to dc converter, usually a buck-boost converter, which stores excess energy to provide power when needed. High power quality is maintained by a PI controller, which guarantees steady voltage and current for both DC and AC loads. With filtering components to guarantee smooth operation, the system is connected to the grid via a three-phase VSI and an islanding switch. This decentralized approach improves flexibility, scalability, and energy flow optimization while ensuring seamless integration with the grid.

4. Control Algorithms

In this work, totally three control algorithms are imployed

Through the use of an MPPT algorithm, which is used in the SEPIC block, to regulate the Maximum Power Point Tracking acquired from the PV array. By managing the battery's current and the direct current voltage that MPPT determines with the assistance of the BESS unit's PI Controller. Inverter control, which synchronizes the PV system to the grid to supply AC power whenever there is a greater demand for it and maintains a constant dc bus voltage under fluctuating loads.

4.1 MPPT Control Method

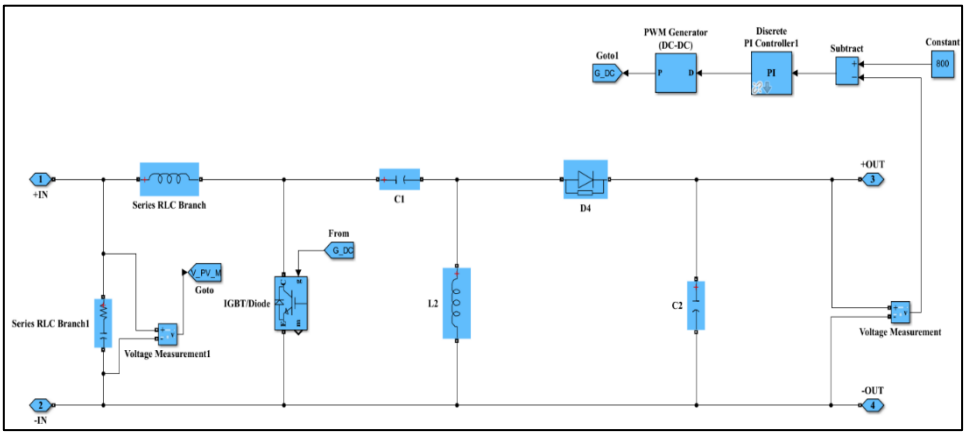

Figure 6. MPPT Control Method

A series RLC branch, which acts as a filter to smooth the input current, receives the solar panel's output power as input in Figure 6 for the MPPT control technique. The SEPIC (Single-Ended Primary Inductor Converter), a DC-DC converter made up of two inductors, a coupling capacitor, diodes, and a MOSFET/IGBT switch, receives the input after that. The inductors can stack power because the switch closes when it is in the on state. A coupling capacitor is used to deliver the stacked power for output when the switch is in the OFF condition, ensuring a steady DC output voltage. The discrete PI controller receives error signals from the subtraction of the measured output voltage value from the voltage measurement block and the fixed constant, set point, or reference value.In order to reduce the error between a desired set point and the actual system output, a proportional integral controller is a feedback mechanism of control method that is frequently used in areas. In order to address persistent discrepancies, it combines two components: the integral term (I), which adds the error value over time, and the proportional term (P), which produces a response relative to the error. In order to maintain system stability, PI controllers are widely used to control variables like voltage or current. The PWM Generator receives the error-free signals from the PI controller's output and transforms them into a PWM signal to regulate the switching behavior of the IGBT. The IGBT switch receives these gate pulses, allowing the maximum power from thesolar panel.

4.2 Bess Unit Control Method

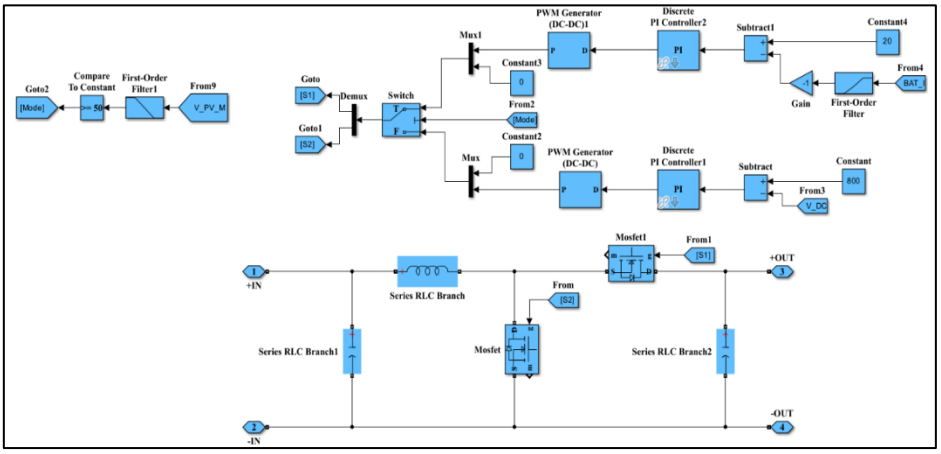

Figure 7. Battery Control Method

The output of the MPPT is used as input to the bidirectional dc-dc converter in Figure 7 for the control of the Battery Energy Storage System (BESS) unit. The output is then used as input to the battery, which is a Lead-Acid battery type with a rated capacity of 10 Ampere-hour and an operating voltage of 420 volts. The battery response time is 30 seconds, and its initial state of charge is stated as 80%. The first order filter, a low-pass filter that improves gain by permitting low frequency components and filters out voltage or current harmonics to preserve system stability, receives the battery current. The battery output current is subtracted and compared to a fixed set point value. When the PI controller receives these error signals, the steady state errors—the discrepancy between the intended and actual outputs—are removed, stabilizing the system. The PWM generator then drives these signals to produce PWM pulses, which are then sent to the switch to monitor the battery current along with a reference value. Next, a comparison is made between the desired output and the DC output voltage. The PI controller receives these error signals once more, and the PWM generator transforms them into PWM pulses by feeding the error-free signals from the PI controller's output. To keep an eye on the battery voltage, the switch receives these gate pulses in addition to the reference value. As a result, the BESS unit provides the power to balance the system and satisfy demands when they exceed supply from solar PV panels.

4.3 Inverter Control Method

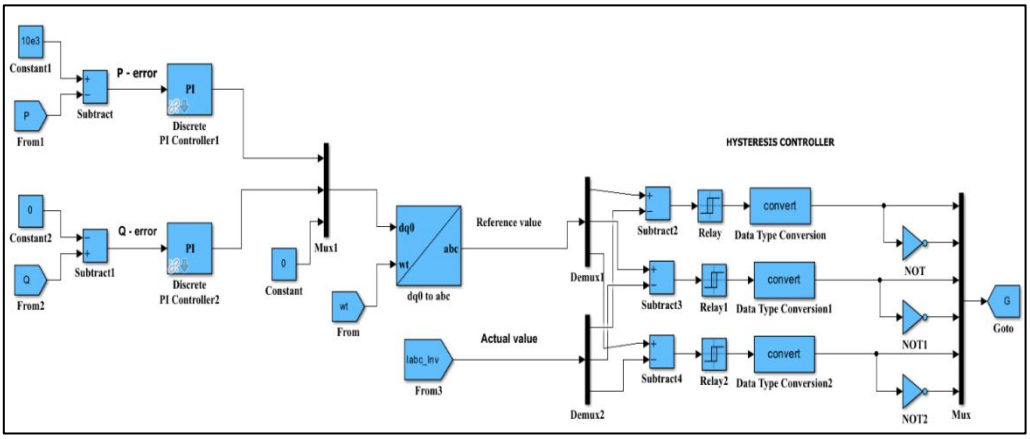

Figure 8. Inverter Control Method Using Hysterisis Controller

Real power and reactive power are considered for inverter control in Figure 8, where the reactive power is set to zero. Real power is calculated by subtracting the setpoint value from the measured output power values. Reactive power is calculated by subtracting the setpoint value from the measured output values. The PI controller receives the real and reactive power error signals from these processes, which are then sent to the mux. The value wt is obtained from the Phase Locked Loop (PLL), which helps synchronize the PV system with the utility grid.The output from mux is sent to the Park transformation block, which uses the inverse park transformation method to phase shift the dq0 axis (rotating reference frame) at a 120-degree angle and convert it to a three-phase abc angle. Demux receives both the reference value from the inverse transformation block and the actual value from the 3-phase inverter current (Iabc). A hysterisis controller is used to regulate the inverter's output. Values are fed into the relay for switching operations after the demux's output is subtracted. Relay switching operations are 0.0001 for ON conditions and -0.0001 for OFF conditions.To compare the output values and obtain the desired output, the relay switching operations' output is sent to the data type conversion block and then to the NOT logical operator. The grid receives this output, and the three-phase grid voltage and current are measured.

5. Simulation Model

Matrix Laboratory Simulink, a flexible platform for mathematical modeling, computation, and visualization, is used in this work to conduct experiments. It works well for processing signals and solving challenging issues.

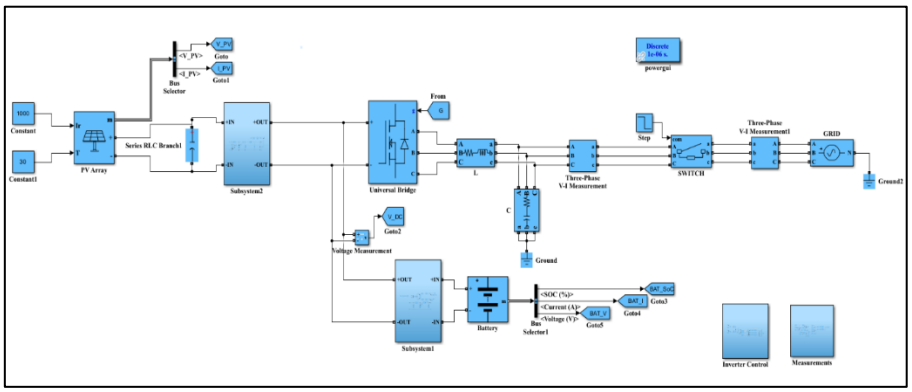

Figure 9. Simulation Model For Decentralized Control Strategy

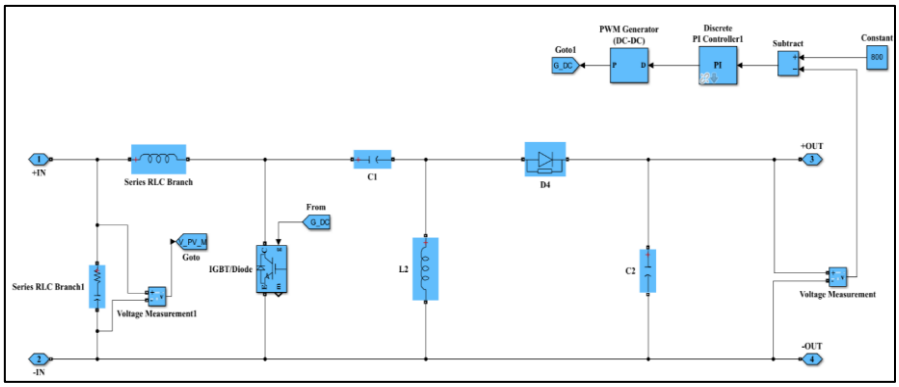

Figure 10. Subsystem Model for Sepic Converter

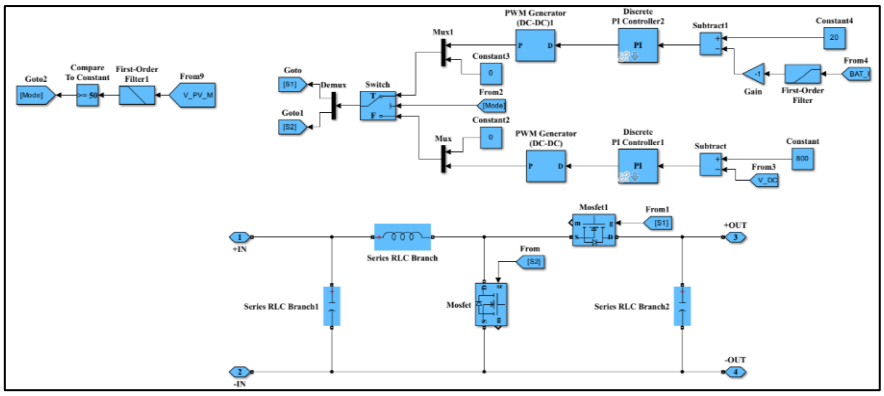

Figure 11. Subsystem Model for Bidirectional Dc-Dc Converter

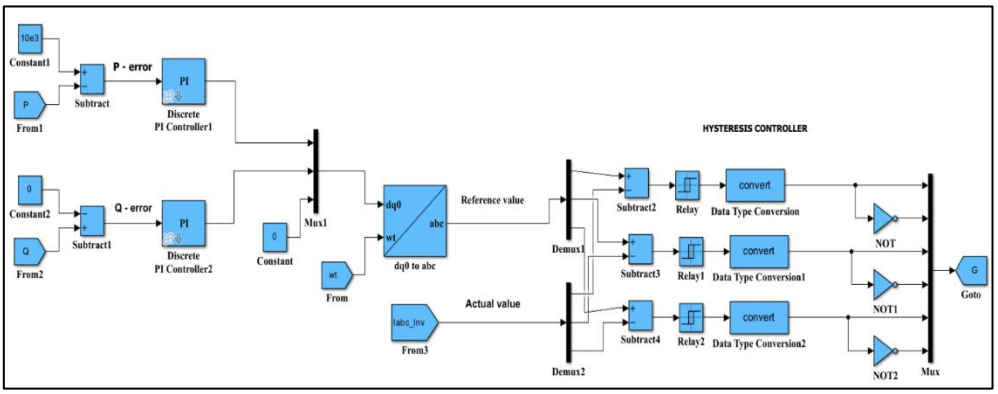

Figure 12. Subsystem Model for Inverter Control

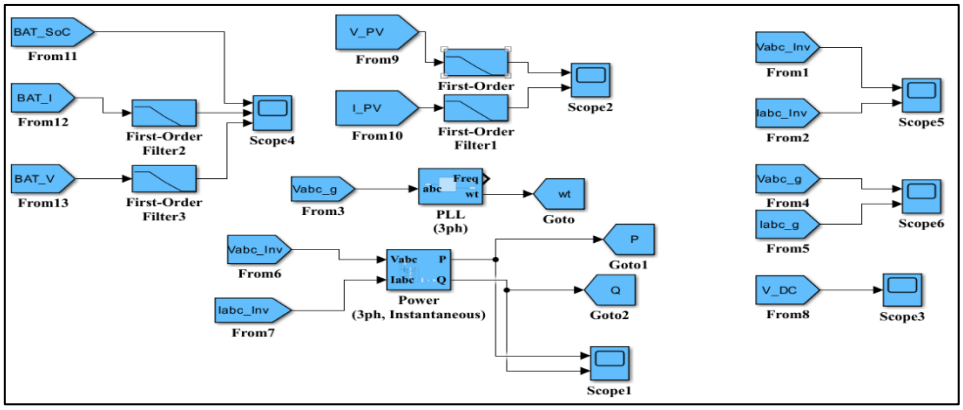

Figure 13. Subsystem Model for Measurements Block

6. Simulation Results and Discussion

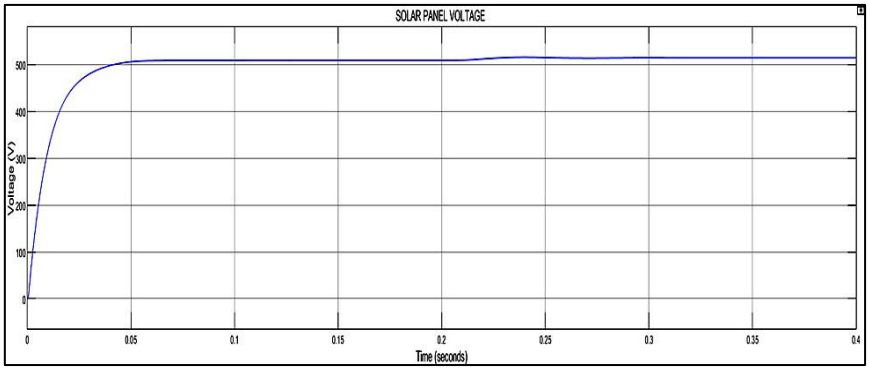

Figure 14. Solar Panel Voltage

A solar panel's voltage is displayed in Figure 14. The voltage initially increases rapidly from 0 to roughly 500V before remaining constant. This indicates that the panel is transitioning

from startup to regular operation. As is typical of high-power solar systems, the system stabilizes in 0.4 seconds. According to the graph, the control system is made to swiftly stabilize the output voltage.

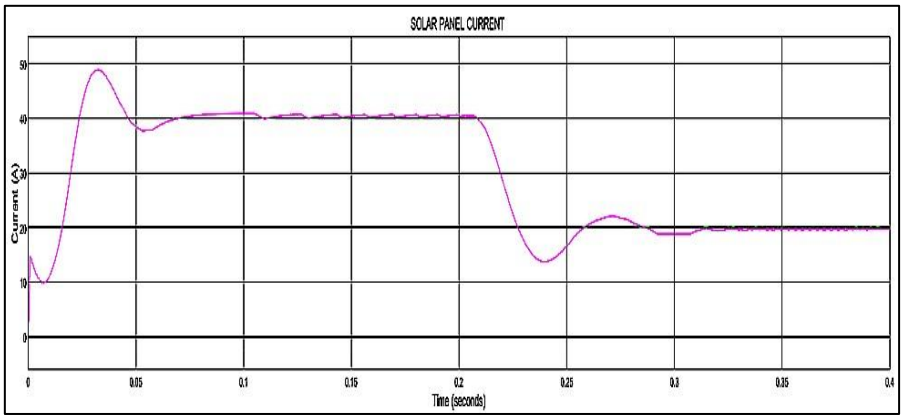

Figure 15. Solar Panel Current

The solar panel's current is displayed in Figure 15. Within the first 0.02 seconds, it rapidly increases from zero to roughly 50 A. When the system starts up or connects to a load, inrush current may be the cause of this abrupt increase. The system is adjusting as the current decreases and exhibits slight oscillations between 0.02 and 0.25 seconds after the peak. The system reaches a stable state when the current stabilizes at about 40 A after 0.25 seconds.

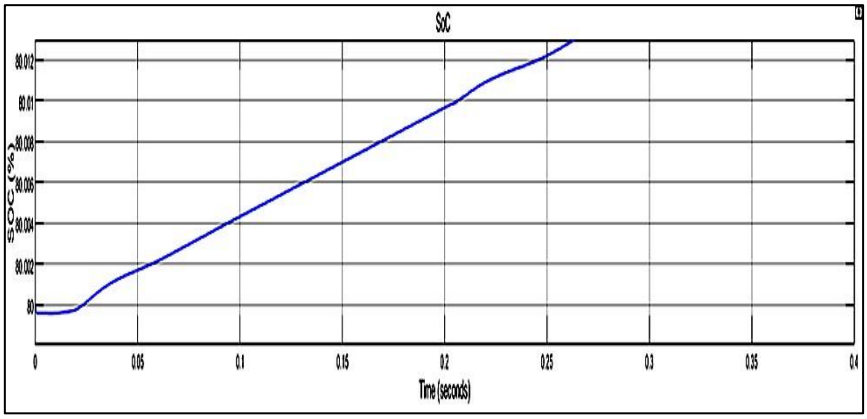

Figure 16. Battery SoC

The battery's State of Charge (SoC) is displayed in Figure 16. The battery is initially partially charged, starting at about 80%. After that, the SoC gradually rises, indicating that the battery is charging steadily. This consistent increase indicates that the charging current is under control.

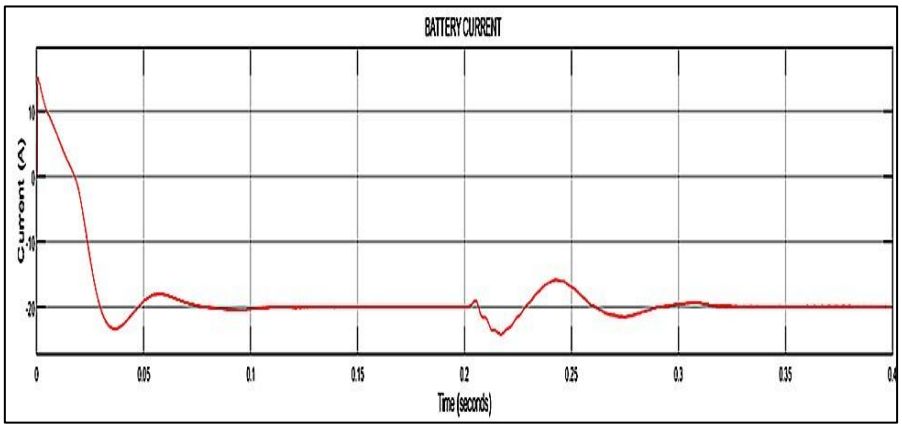

Figure 17. Battery Current

The battery current is displayed over time in Figure 17. It rapidly drops to -20 A after beginning at a positive 10 A. This indicates that the battery starts charging before switching to discharging. The current varies slightly between 0.05 and 0.15 seconds, indicating that the system is settling following a sudden change. The battery is steadily discharging after 0.15 seconds, as evidenced by the current remaining at about -20 A with minor ripples.

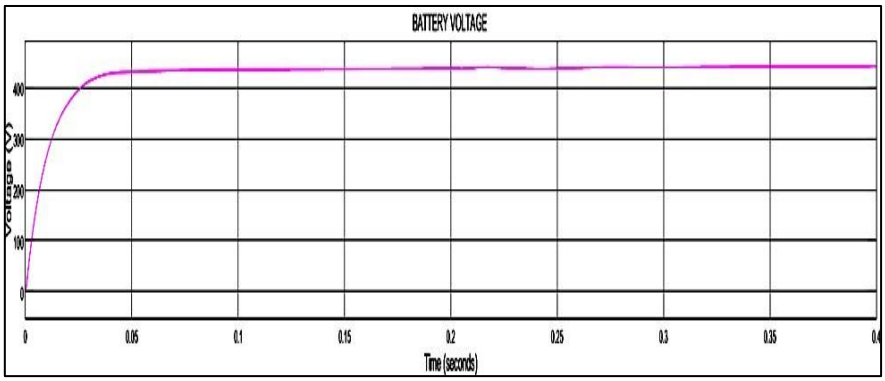

Figure 18. Battery Voltage

The battery voltage is displayed in Figure 18. Between 0 and 0.05 seconds, it rapidly increases from 0 to roughly 400V, indicating that either a voltage source is applied or the battery is charging. Following this brief increase, the voltage modifies a little before stabilizing between 0.05 and 0.15 seconds. This occurs as a result of the control system controlling the voltage or the internal behavior of the battery. The voltage remains constant with very slight variations after 0.15 seconds, indicating that the battery is operating steadily.

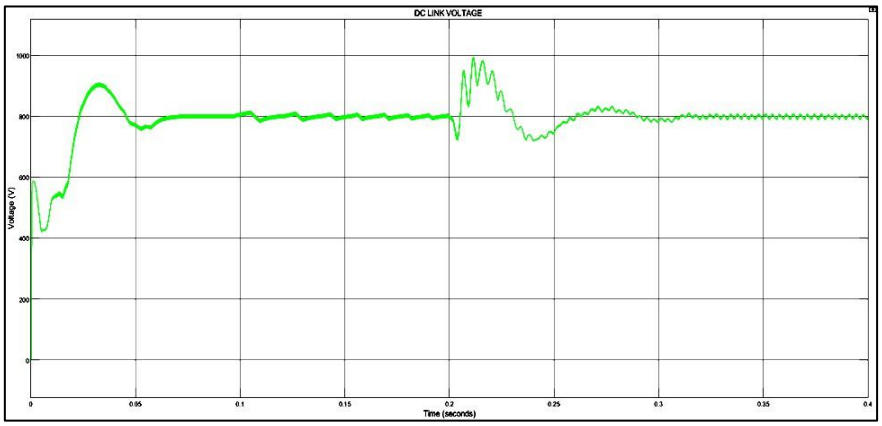

Figure 19. DC Link Voltage

The DC Link voltage is displayed in Figure 19. Between 0 and 0.05 seconds, it rapidly increases from 0V to roughly 800V. This occurs when the voltage source is applied or the DC link capacitor is charging. Following that, as the system corrects and stabilizes between 0.05 and 0.2 seconds, the voltage fluctuates around 800V. The power source behavior, control switching, or abrupt changes in load could be the cause of the 0.2-second peak oscillations.

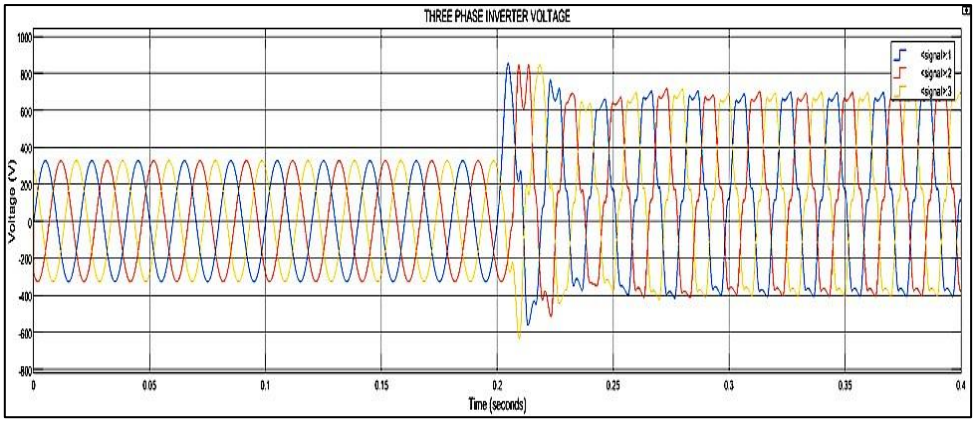

Figure 20. Three Phase Inverter Voltage

The three-phase inverter voltage is displayed in Figure 20. The three waveforms are initially equal in size, smooth, and 120° apart, which is typical for a balanced system between 0 and 0.2 seconds. The inverter is generating AC power, as evidenced by the voltage peaking at around ±400 V. The waveforms briefly become erratic at 0.2 seconds and then continue to do so until 0.25 seconds. A sudden change in load, control actions, or switching within the inverter could be the cause of this disturbance.

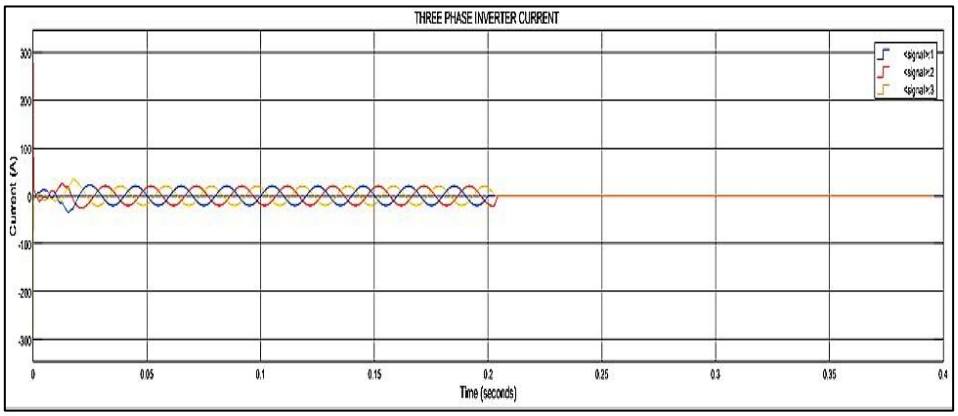

Figure 21. Three Phase Inverter Current

The three-phase current is depicted in Figure 21. As is typical for a balanced system between 0 and 0.2 seconds, the three waveforms are initially equal, smooth, and shifted by 120° from one another. The inverter is generating AC current, as evidenced by the currents peaking at around ±400 V. The waveforms briefly become erratic at 0.2 seconds and then continue to do so until 0.25 seconds. A sudden change in load, a control action, or an internal switch within the inverter could be the cause of this. The waveforms exhibit high-frequency switching with increased noise after 0.25 seconds, which is typical when the inverter's output is controlled by pulse-width modulation (PWM).

Figure 22. Three Phase Grid Voltage

The three-phase grid voltage is displayed in Figure 22. Each phase's RMS value is 230 V, and the three voltage waves are smooth with peaks of roughly ±325 V. As is common for a balanced three-phase system, the waves are 120° apart. This phase shift is evident due to the

colors red, blue, and yellow. Throughout the full 0.4 seconds, the voltage remains constant in both size and frequency, indicating that the grid voltage is stable.

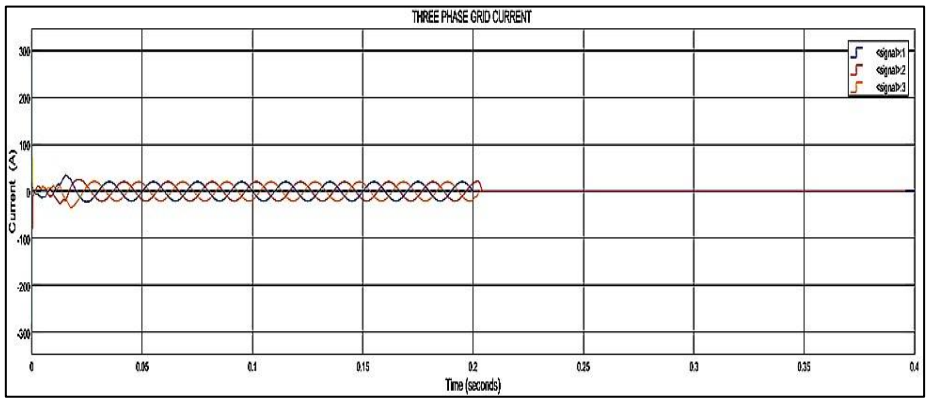

Figure 23. Three Phase Grid Current

The three-phase grid current is depicted in Figure 23. The three current waves are initially smooth and shifted by 120°, which is typical for a balanced system in the 0–0.1 second range. During this period, the current peaks at roughly ±100 A. The currents gradually decrease to zero after 0.1 seconds. There is no current flowing after 0.2 seconds, indicating that the system is either disconnected or not loaded.

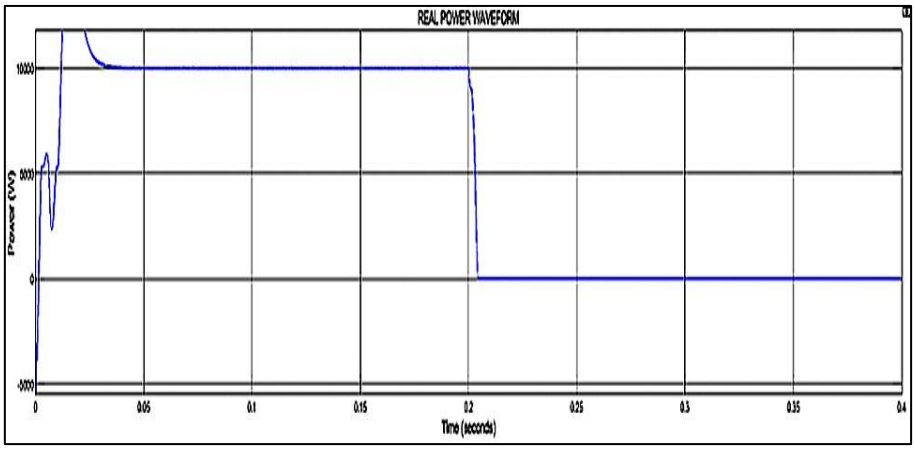

Figure 24. Real Power

The actual power over time is depicted in Figure 24. When the system first boots up or the load fluctuates between 0 and 0.02 seconds, the power fluctuates a little. After that, it operates steadily for 0.02 to 0.2 seconds, settling at roughly 10 kW. The power abruptly cuts to zero at about 0.2 seconds. This indicates that the system ceased to provide active power,

most likely as a result of the system shutting down or the load being disconnected. After that, the circuit doesn't actually have any power flow.

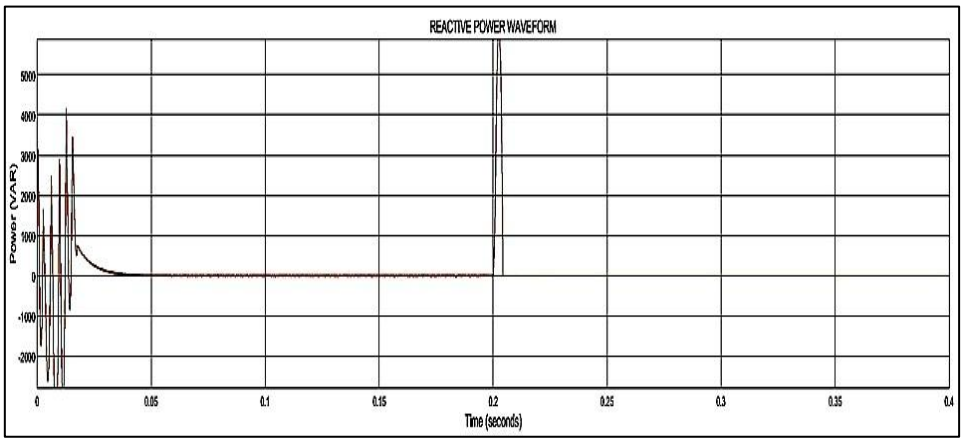

Figure 25. Reactive Power Waveform

Reactive power is plotted over time in Figure 25. Reactive power fluctuates between positive and negative values at first, but these fluctuations diminish and go away after around 0.02 seconds. This occurs as a result of a load connection or system startup. The system is operating with low reactive power, or close to unity power factor, after that, as the reactive power remains near zero for 0.02 to 0.2 seconds. Reactive power eventually falls to zero and remains there, most likely indicating that the load or system was disconnected.

6.1 Limitations and Challenges

Voltage Deviation: The most common decentralized control method is droop control. It lets devices share power automatically but causes the voltage to change slightly from its normal value, especially when the load changes.

Slow Transient Response: Droop control methods can respond slowly to sudden changes in load or power generation. To improve current sharing and voltage regulation, increasing the droop coefficient helps, but it also causes larger voltage drops. To solve this, a PI controller is used in this work. It removes the error between the measured and desired output values. The corrected signal is sent to a PWM generator, which creates PWM pulses. These pulses control the IGBT or MOSFET switches to maintain stable output and improve system performance.

Limited Awareness: In a decentralized system with dispersed energy resources, the converter functions autonomously and can only access its local measurements, such as output voltage and current. The state of charge of every BESS unit is a difficult component that prevents the system from operating at its best due to a lack of global information about the microgrid's condition, such as total operating loads. The SoC of BESS units is also unknown to distributed generating units. Because of this, it is challenging to determine whether the BESS unit is charged enough to support the microgrid

Robustness Problems: It is difficult and complex to design decentralized controllers that can withstand a variety of circumstances, including changes in load and plug-and-play capabilities of distributed generating units that add or remove sources.

6.2 Advantages of the Proposed System

No Single Point of Failure: In contrast to centralized systems, which rely on a single master controller to manage the entire system, decentralized systems operate using local measurements and data gathered from the controller. They also lack a single component that could bring down the entire microgrid in the event of a failure. DEcreased Communication Failure: By running the DG units separately, the system becomes more resilient. This reduces communication delays and the possibility of a communication link failure, which could cause instability in the system, by requiring little to no real-time communication between the DG units.

Silent Integration: The microgrid can readily accommodate new distributed generators and loads, and it adjusts to these changes by controlling voltage and preserving current sharing in a decentralized system without necessitating intricate controller reconfigurations or modifications. Each DG unit or load can be simply "plugged in or plugged out" based on supply and demand because its local controllers will automatically adjust its operation based on local bus voltage.

Simple Control Algorithms: Because decentralized systems rely on local controllers, they necessitate comparatively straightforward local control loops, which makes controller implementation and design easier.

Self-Healing Capabilities: The decentralized system can self-correct to preserve stability and power balance in the event of slight disruptions or changes.

7. Conclusion And Future Scope

A complex decentralized energy management system that successfully combines a photovoltaic system with energy storage and grid interaction is presented in this work. Energy generation, storage, and distribution across DC and AC loads are all optimized by the system's design. The main parts of this system are a bidirectional DC-DC converter that facilitates effective energy flow between the system and energy storage devices like batteries, an MPPT algorithm that guarantees maximum energy harvesting from the PV system, and a SEPIC converter that controls voltage regulation. To maintain ideal system performance, a PI controller is used to guarantee steady voltage and current levels. The system has a three-phase voltage source inverter and an islanding switch to increase efficiency and guarantee smooth integration with the electrical grid. In order to detect grid failures or disturbances, disconnect the decentralized system from the grid, and function independently if required, an islanding switch is essential. In order to contribute to the overall stability and resilience of the grid, the three phase VSI makes sure that energy exchanges smoothly and steadily between centralized grid systems and decentralized power sources, such as the PV system. The overall dependability and resilience of the energy infrastructure are increased by permitting autonomous operation during grid disruptions, which enables the system to sustain a continuous power supply even in the case of grid failures. By maximizing the use of renewable energy sources like solar and wind for energy generation and storage, the system also lessens reliance on the centralized grid. Because it lessens reliance on non-renewable energy sources, this decrease in grid dependence also helps the system's environmental sustainability.

References

[1] Dragičević, Tomislav, Xiaonan Lu, Juan C. Vasquez, and Josep M. Guerrero. "DC microgrids—Part II: A review of power architectures, applications, and standardization issues." IEEE transactions on power electronics 31, no. 5 (2015): 3528-3549.

[2] Arani, AA Khodadoost, G. B. Gharehpetian, and M. Abedi. "Review on energy storage systems control methods in microgrids." International journal of electrical power & energy systems 107 (2019): 745-757.

[3] Fu, Qiang, Adel Nasiri, Vijay Bhavaraju, Ashish Solanki, Tarek Abdallah, and David C. Yu. "Transition management of microgrids with high penetration of renewable energy." IEEE Transactions on Smart Grid 5, no. 2 (2013): 539-549.

[4] Pourbehzadi, Motahareh, Taher Niknam, Jamshid Aghaei, Geev Mokryani, Miadreza Shafie-khah, and João PS Catalão. "Optimal operation of hybrid AC/DC microgrids under uncertainty of renewable energy resources: A comprehensive review." International journal of electrical power & energy systems 109 (2019): 139-159.

[5] Strunz, Kai, Ehsan Abbasi, and Duc Nguyen Huu. "DC microgrid for wind and solar power integration." IEEE Journal of emerging and selected topics in Power Electronics 2, no. 1 (2013): 115-126.

[6] Nabatirad, Mohammadreza, Reza Razzaghi, and Behrooz Bahrani. "Decentralized voltage regulation in islanded DC microgrids in the presence of dispatchable and non-dispatchable DC sources." In 2020 22nd European Conference on Power Electronics and Applications (EPE'20 ECCE Europe), IEEE, 2020, 1-10.

[7] Azizi, Ali, Saeed Peyghami, Hossein Mokhtari, and Frede Blaabjerg. "Autonomous and decentralized load sharing and energy management approach for DC microgrids." Electric Power Systems Research 177 (2019): 106009.

[8] Yang, Qiang, Le Jiang, Hailin Zhao, and Hongmei Zeng. "Autonomous voltage regulation and current sharing in islanded multi-inverter DC microgrid." IEEE Transactions on Smart Grid 9, no. 6 (2017): 6429-6437.

[9] Nabatirad, Mohammadreza, Reza Razzaghi, and Behrooz Bahrani. "Decentralized energy management and voltage regulation in islanded DC microgrids." IEEE Systems Journal 16, no. 4 (2022): 5835-5844.

[10] Nabatirad, Mohammadreza, Reza Razzaghi, and Behrooz Bahrani. "Decentralized voltage regulation in islanded DC microgrids based on a modified droop control using superimposed AC voltage." Authorea Preprints (2021).

[11] Dam, Duy-Hung, and Hong-Hee Lee. "A power distributed control method for proportional load power sharing and bus voltage restoration in a DC microgrid." IEEE transactions on industry applications 54, no. 4 (2018): 3616-3625.

[12] Kumar, Jaynendra, Anshul Agarwal, and Nitin Singh. "Design, operation and control of a vast DC microgrid for integration of renewable energy sources." Renewable Energy Focus 34 (2020): 17-36.

[13] Ravada, Bhaskara Rao, and Narsa Reddy Tummuru. "Control of a supercapacitor-battery-PV based stand-alone DC-microgrid." IEEE Transactions on Energy Conversion 35, no. 3 (2020): 1268-1277.

[14] Tucci, Michele, Stefano Riverso, Juan C. Vasquez, Josep M. Guerrero, and Giancarlo Ferrari-Trecate. "A decentralized scalable approach to voltage control of DC islanded microgrids." IEEE Transactions on Control Systems Technology 24, no. 6 (2016): 1965-1979.

[15] Setiawan, Made Andik, Ahmed Abu-Siada, and Farhad Shahnia. "A new technique for simultaneous load current sharing and voltage regulation in DC microgrids." IEEE Transactions on Industrial Informatics 14, no. 4 (2017): 1403-1414.

[16] Nabatirad, Mohammadreza, Reza Razzaghi, and Behrooz Bahrani. "Decentralized voltage regulation and energy management of integrated DC microgrids into AC power systems." IEEE Journal of Emerging and Selected Topics in Power Electronics 9, no. 2 (2020): 1269-1279.

[17] Al-Ismail, Fahad Saleh. "DC microgrid planning, operation, and control: A comprehensive review." IEEe Access 9 (2021): 36154-36172.